

609-51

APOLLO LUNAR SOUNDER DIGITAL  
DATA DECONVOLUTION

June 1973

JET PROPULSION LABORATORY  
CALIFORNIA INSTITUTE OF TECHNOLOGY  
PASADENA, CALIFORNIA

609-51

APOLLO LUNAR SOUNDER DIGITAL  
DATA DECONVOLUTION

June 1973

Rolando Jordan

Approved by

*Walter E. Brown Jr.*

Walter E. Brown, Jr.  
Principal Investigator (S209)

JET PROPULSION LABORATORY  
CALIFORNIA INSTITUTE OF TECHNOLOGY  
PASADENA, CALIFORNIA

CONTENTS

1.0	INTRODUCTION . . . . .	1
2.0	DESCRIPTION OF THE PROCEDURE . . . . .	1
3.0	PHASE ERROR DETECTION PROCEDURE . . . . .	5
3.1	Dispersion Constant Measurements . . . . .	6
3.1.1	Procedure . . . . .	6
3.1.2	Accuracy Requirements . . . . .	7
3.1.3	Measurement Accuracies . . . . .	7
3.2	Phase Detection and Roll Back . . . . .	9
4.0	CONCLUSIONS . . . . .	17

## FIGURES

1.	Response of Various Filters to Input Echo . . . . .	8
2.	Image Dissector Trace of a Doppler Matched Filtered Nonlinear Signal. . . . .	10
3.	Microdensitometer Trace of a Doppler Filtered Linear Signal Record. . . . .	12
4.	Typical Signal Record Power Spectrum . . . . .	13
5.	Typical Signal Record Phase Spectrum . . . . .	14
6.	Typical Signal Record Phase Spectrum after Quadratic Phase Correction . . . . .	15
7.	Typical Signal Record after Pulse Compression. . . . .	16
8.	Typical Phase Spectrum after Quadratic Phase Correction and Initial Phase Rollback. . . . .	18
9.	Typical Phase Spectrum after Quadratic Phase Correction and Rotation. This Spectrum is Ready for the Stacking Operation . . . . .	19
10.	System Phase Error Function . . . . .	20
11.	System Sidelobe Response with $\text{Sinc}^2$ Weighting. . . . .	21
12.	Radar Data Parameter Tabulation. . . . .	22
13.	Relative Amplitude Spectrum of HF1 ALSE Data (Start of FT01) . .	23
14.	ALSE HF1 System Relative Amplitude Spectrum . . . . .	24
15.	System Sidelobe Response . . . . .	25
16.	$\text{Sinc}^2$ Weighted System Sidelobe Response after Performing a Sinc Squared Weighting Operation. . . . .	26
17.	Ideal System Sidelobe Response . . . . .	27
18.	Pulses Stacked = 1 . . . . .	29
19.	Pulses Stacked = 64 . . . . .	30
20.	Pulses Stacked = 512 . . . . .	31

## 1.0 INTRODUCTION

The purpose of the work reported on herein was to demonstrate the possibility of enhancing the subsurface feature detection probability by digital processing and filtering.

This report describes a procedure developed which calculates the system phase errors of the Apollo 17 Lunar Sounder hardware from the signal as recorded on the signal film. It is important to determine these phase errors because they give rise to system sidelobes. System sidelobes must be low so that they will not mask subsurface echoes in close proximity to the strong specular return coming from the surface reflection. Factors that cause these system phase errors are hardware deficiencies that result in non-linear transfer functions throughout the radar system, optical recorder, film characteristics and the optical correlator.

The cost of detecting and correcting these deficiencies is beyond the scope of the present hardware development program.

## 2.0 DESCRIPTION OF THE PROCEDURE

The signal film from the Lunar Sounder experiment contains information from a large number of weaker echoes plus a strong specular return. After the transmitted signal is reflected from the lunar surface and received by the antenna, the radar signal is amplified by the receiver. At this point, the signal waveform has the form

$$e(t) = \sum_n a_n(t) \exp \left[ j \left( \omega_c (t - t_n) + K(t - t_n)^2 \right) \right]$$

The signal, at this point, is mixed with a coherent oscillator waveform for down conversion and upon filtering, the signal, assumes the form

$$e(t) = \sum_n a_n(t_n) \exp \left[ j \left( (\omega_c - \omega_1)(t - t_n) + K(t - t_n)^2 \right) \right]$$

where  $a_n$  is the amplitude of each return,  $\omega_c$  is the frequency of the radar carrier,  $\omega_e$  is the receiver coherent oscillator frequency and  $K$  is the system dispersion constant resulting from the linear chirp and  $t_n$  is the delay of the return from the Nth reflector. The return signal may also be represented by

$$e(t) = \int A(\omega) \exp \left[ j(\phi(\omega) - \omega t) \right] d\omega$$

where  $A(\omega)$  and  $\phi(\omega)$  are the amplitude and phase terms of the transform of the function characterizing  $e(t)$ . Within the radar and recording media this signal undergoes through a network whose transfer function is characterized by an amplitude transfer function  $B(\omega)$  and a phase error  $\phi_e(\omega)$  and consequently the output signal now takes the form

$$o(t) = \int A(\omega) * B(\omega) \exp \left[ j(\phi(\omega) - \phi_e(\omega) - \omega t) \right] d\omega$$

The system characteristics  $B(\omega)$  and  $\phi_e(\omega)$  are those which introduce errors to the spectral characteristics of the return and consequently give rise to unwanted returns when excited by a strong input pulse. These undesirable returns are known as the system sidelobes. These sidelobes may be calculated by looking at the output of the system when the return signal entering the antenna is frequency independent, for example, a specular echo. For this case  $A(\omega)$  can be any constant value (unity) and the phase term zero. An impulse function satisfies these criteria. Thus, when the system is excited by an impulse function, the output of the system has the form

$$o(t) = \int_{-\infty}^{\infty} B(\omega) \exp \left[ j(\phi_e(\omega) - \omega t) \right] d\omega$$

If the frequency content of the device exciting the lunar surface and system is limited to a given band of frequencies, the integration of the above integral becomes bounded or

$$o(t) = \int_{\omega_1}^{\omega_2} B(\omega) \exp[j(\phi_e(\omega) - \omega t)] d\omega$$

This equation, then represents the impulse response of the unweighted system. Since the response of a perfect system to this function ( $A(\omega) = 1.0$  and  $\phi(\omega) = 0$ ) is

$$o_p(t) = \int_{\omega_1}^{\omega_2} \exp(-j\omega t) d\omega$$

it becomes desirable to pass the signal through a filter whose amplitude spectral response  $C(\omega)$  is  $C(\omega) = 1/B(\omega)$  and its phase response  $\phi_c(\omega)$  is  $\phi_c(\omega) = -\phi_e(\omega)$ . Consequently, it becomes necessary to measure the system spectral characteristics ( $B(\omega)$  and  $\phi_e(\omega)$ ) to a high degree of precision in order to "construct" a filter which can compensate for systematic errors. This filter would take the form of a software frequency domain function.

The transmitted waveform does not represent a perfect impulse function but contains a built-in quadratic phase function as well as amplitude and phase errors. Since it is not required to separate the transmitted waveform from the system response but only the surface characteristics from the system response, the errors (amplitude and phase) of the transmitted waveform may be lumped into the system response. The quadratic phase function of the transmitted waveform is used to disperse the transmitted energy over a long period of time, consequently lowering the peak transmitted power to 1/128 of the effective peak power of the waveform. This technique is known as pulse compression. This quadratic phase function is expected to take the form

$$\phi_d(\omega) = m(\omega - \omega_o)^2 + \phi_e(\omega)$$

where  $m$  is a constant,  $\omega_o$  is the reference frequency and  $\phi_e(\omega)$  is a phase error function describing all the higher and lower order terms than the quadratic. Since it will not be possible to determine the constant  $m$  exactly, the above equation may be expressed by

$$\phi_d(\omega) = N(\omega - \omega_o)^2 + \phi_f(\omega)$$

where  $N$  is the estimated value of  $m$  and  $\phi_f(\omega)$  contains a quadratic term as well, to compensate for the error in the assumed value  $n$  for the constant  $m$ . In summary, the amplitude as well as phase errors contributed by the transmitted waveform may be lumped into the overall system transform function without loss of generality provided the medium (space) is non-dispersive as well as having a surface with frequency independent reflectivity.

The presence of multiple reflectors will cause constructive and destructive interference of the return waves dependent on the temporal spacing of these reflectors. This interference of returns requires that the amplitude spectra of the system be obtained only by analyzing the spectra from a large number of returns from different locations in order to average out the effects of this random interference on the amplitude spectra.

The detection of the phase error function of the system poses a more complicated procedure than that for detecting the system amplitude spectral response characteristics. Since the phase error spectrum corresponds to the phase of the output waveform when the system is excited by a monochromatic waveform of zero phase and the system is never excited in this manner, a more complicated procedure is used. The procedure assumes that the return primarily comes from a single strong reflector and added to it are returns from weaker secondary reflectors as well as additive noise. Furthermore, the signal has gone through slight nonlinear components prior to its analysis. The echo from this signal return is expanded into Fourier series expansion so that it may be represented by the summation of a large number of constant amplitude sinusoids, each with a phase term. The source of the return is then located to an accuracy consistent with the signal-to-noise of the return. The return is then translated in time to the origin and the phase of these vectors (sinusoids) computed. The resultant phase spectrum  $\phi(\omega)$  is

$$\phi(\omega) = m(\omega - \omega_o)^2 + \phi_e(\omega) + \phi_r(\omega) + \phi_n(\omega)$$



where  $\phi_m(\omega - \omega_o)$  represents the ideal quadratic phase function (frequency dispersion),  $\phi_e(\omega)$  represents the system phase error function,  $\phi_r(\omega)$  the phase shift due to secondary returns and  $\phi_{re}(\omega)$  the phase shift due to noise.

Since we may substitute for the quadratic phase function plus its error, the above expression may be replaced by

$$\phi(\omega) = N(\omega - \omega_o)^2 + \phi_f(\omega) + \phi_e(\omega) + \phi_r(\omega) + \phi_n(\omega)$$

Subtracting from this phase spectra the assumed quadratic phase function and combining  $\phi_f(\omega)$  and  $\phi_e(\omega)$  we get

$$\phi_s(\omega) = \phi_e(\omega) + \phi_r(\omega) + \phi_n(\omega)$$

where  $\phi_s(\omega)$  is the phase function to be "stacked." We may combine the function  $\phi_f(\omega)$  and  $\phi_e(\omega)$  into a single function because they both represent phase errors and we are only interested in their sum and not the individual functions.

If this procedure is repeated over an area where the phase of the secondary returns are not correlated with the phase of secondary returns from the previous pulse analyzed, then when the phase spectra are added on an ensemble basis, the phase error spectrum will add coherently as it is tied primarily to the phase of the strong return while the phase of the secondary returns are not. Basically, this implies that the secondary returns must move with respect to the surface. Since the phase spectrum of noise is not correlated with the phase of the surface return, when the various phase spectra are added on an ensemble basis, the term arising from noise will add non-coherently. In summary, if the phase of a sufficiently large number of echoes are ensemble averaged, the residual phase spectrum will in the limit approach the system phase error function.

### 3.0 PHASE ERROR DETECTION PROCEDURE

The procedure of taking a signal film, digitizing it and from the digital numbers obtaining the system phase error function and the sidelobes associated with that error is as follows:

1. The dispersion constant of the signals is first obtained.

2. The signal is then Fourier transformed and its amplitude and phase spectra obtained.
3. The phase spectrum is corrected for the effects of dispersion.
4. The phase spectrum (for each frequency) is rolled back to the center of the strongest reflection.
5. If the resultant spectrum has good characteristics, it is saved for an ensemble average operation.

### 3.1 Dispersion Constant Measurements

One of the critical areas in the development of a technique to detect and roll back the phase of each return is that of determination of the dispersion constant of the system. The dispersion constant is defined as follows. The signal on film as recorded by the optical recorder is a summation of signals of the form:

$$e(x) = b_o + \sum_n a_n R_e \left\{ \exp \left[ j\omega_o X + Kx^2 \right] \right\}$$

where  $b_o$  is the film bias,  $a_n$  the amplitude of the returns,  $\omega_o$  the initial frequency of the dispersed signal and  $K$  is the dispersion constant.

Each of these signals represents the return from a reflection facet or scatterer. Because there are a large number of such signals, it can be difficult to obtain an accurate value for the dispersion constant  $K$  from the data. The accuracy required is of the order of 0.5 percent. Because this accuracy requirement exceeds by a large margin the hardware calibration requirements, the only recourse is to use the original signal film for its determination.

#### 3.1.1 Procedure

The procedure used to determine the dispersion constant consists of the following:

1. Using an assumed dispersion constant, obtain a complex filter function.
2. Convolve the signal with the assumed filter junction.

3. Measure the largest value of the filter response.
4. Iterate with a different filter function until the filter response is maximized.

When this is achieved, the dispersion constant which maximizes the output is obtained. This is analogous to locating the focal point of a signal film using coherent light by observing the brightest point. However, because the signal consists of a summation of dispersed signals, this point is not necessarily that which corresponds to the correct dispersion constant. Consequently, a number of different echoes must be observed and their effective dispersion constants measured.

### 3.1.2 Accuracy Requirements

The dispersed pulse is dispersed by approximately 402 radians over the bandwidth used independently of the system. Since the detection of phase errors is to be accomplished by first correcting for the dispersion constant, the corrected phase must lie within  $2\pi$  radians. This corrected phase is the sum of the error in dispersion constant over the bandwidth plus the variation of the phase spectrum about the least squares error fit by a first degree polynomial to the corrected phase spectrum. For most echoes observed this implies an error of 2 or 3 radians over the bandwidth. Thus, an error in the estimation of the dispersion constant of 0.5 percent is tolerable.

### 3.1.3 Measurement Accuracies

A total of 40 echoes were analyzed for their effective dispersion constant. The results have shown a mean value of 5.24 percent below the theoretical perfect system and is well within the system calibration accuracies. The standard deviation of these measurements was 1.1 percent of the mean value. The implications of these measurements is that in order to obtain a value of the dispersion constant sufficiently accurate (0.5 percent) with a low probability of error outside these bounds, a number of echoes should be examined. The practice of evaluating 20 echoes was adopted and a more exact criteria will be obtained later if required. A typical response of an echo to various filters derived of various dispersion constants is shown in Figure 1.

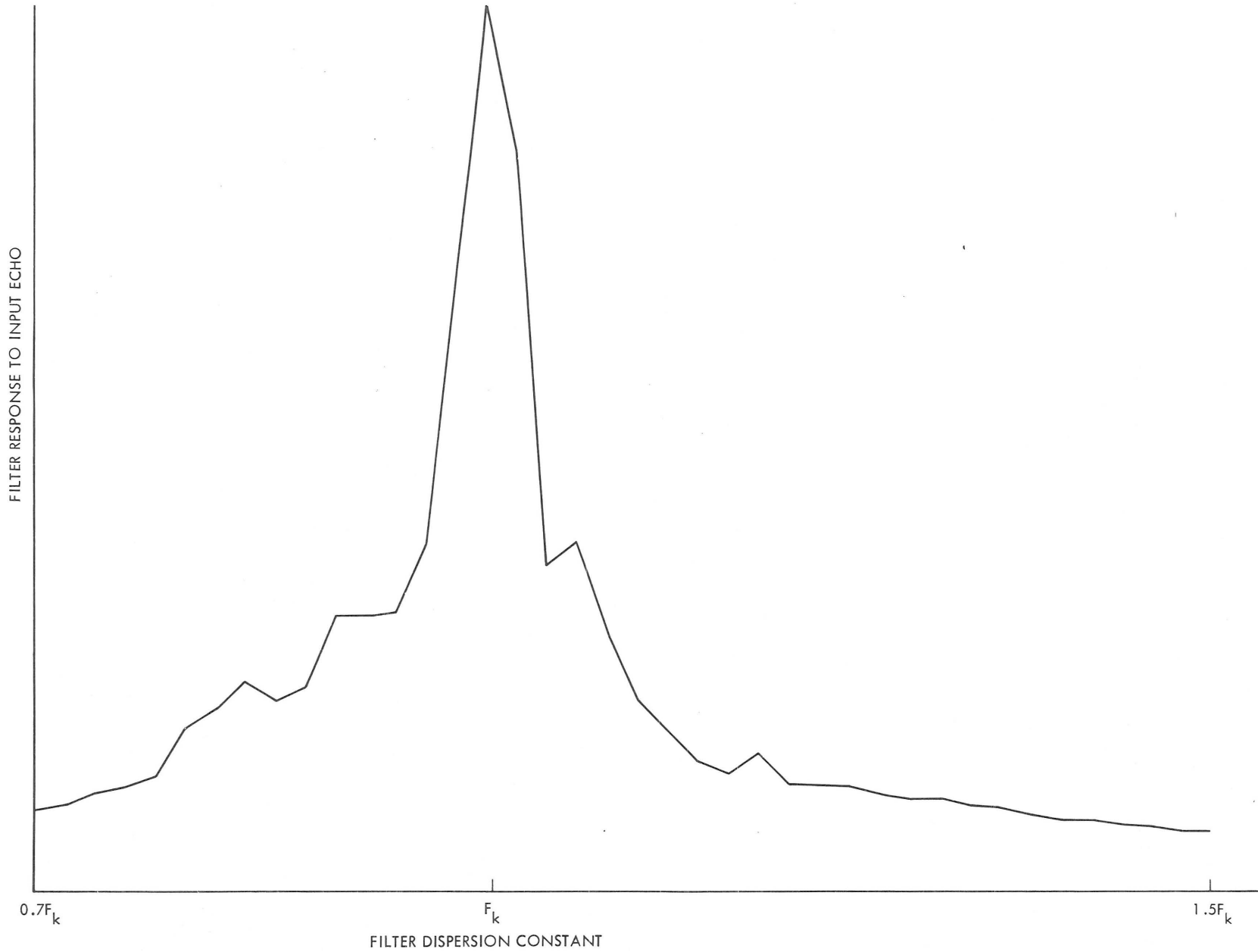


Figure 1. Response of Various Filters to Input Echo

### 3.2 Phase Detection and Roll Back

The data consists of a signal film which contains recorded temporal domain data. This data is presented at the input of the optical recorder and has the form

$$e(t) = \sum_d A_\alpha(t) \operatorname{Re} \left\{ e^{j(\omega_o(t-t_d) + K(t-t_d)^2)} \right\}$$

where  $A_\alpha$  is the amplitude of each return and  $t_d$  the delay of each return.

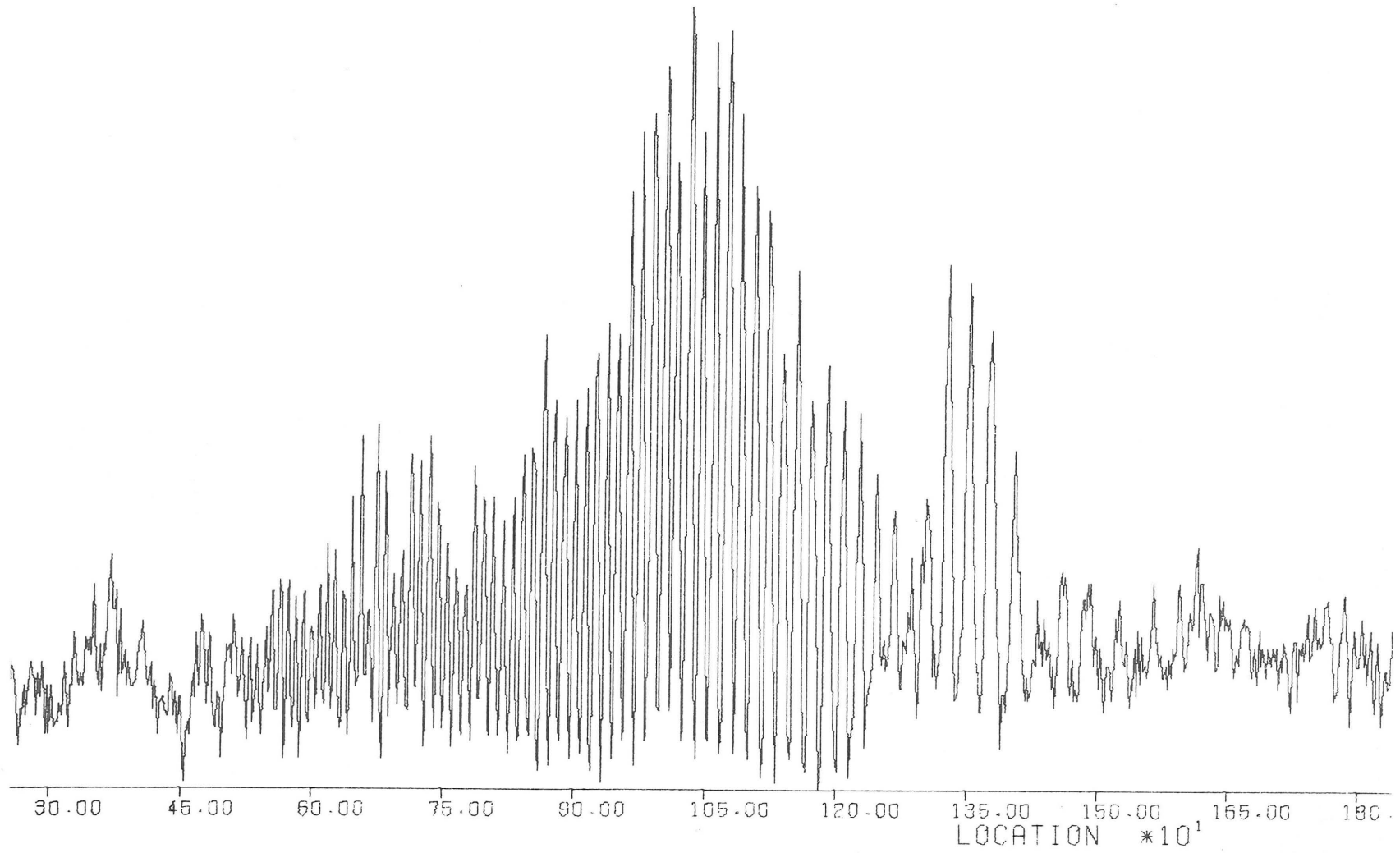
Since the optical recorder records the information on film through a beam deflection which sweeps with some velocity  $v$ , the information on film takes the form

$$e(x) = B_o + B_n(x) + \sum_n C_n(x) \operatorname{Re} \left\{ e^{j\left(\frac{\omega_o}{v}(x-x_n) + \frac{K}{v^2}(x-x_n)^2\right)} \right\}$$

The constant  $B_o$  implies a recording above a bias and  $B_n(x)$  a noise corresponding to the film grain and recorder noise. The data is recorded in the optical recorder film on an ensemble basis and prior to imaging of this data on the image dissector tube; it may be azimuth matched filtered or simply bandpass filtered depending on the azimuth processing desired. However, the signal imaged on the dissector still has this form since no processing is done in the range dimension.

The record which is digitized then has the form shown in the previous equation and is sampled at a rate sufficiently high to preserve the highest desired spatial frequencies without fold over. A spatial filter in the transform plane of the correlator prevents noise outside the desired band of frequencies from folding over and entering at a frequency within the signal pass-band. Figure 2 shows a typical signal film trace of a doppler matched filtered set of echoes but unprocessed in range. The assymetry in the record shows presence of a nonlinearity in the film or optical recorder or analog to digital

10



609-51

Figure 2. Image Dissector Trace of a Doppler Matched Filtered Nonlinear Signal

converter. In Figure 3, another signal film trace where this nonlinearity is not present is shown.

A Fourier Series expansion of this record is then performed and the amplitude and phase spectra obtained. The square of the amplitude spectrum is the power spectrum and a typical power spectrum is shown in Figure 4. The phase spectrum represents the phase of the sinusoid synthesized by performing the Fourier Series expansion with respect to a cosine wave of that frequency. A typical phase spectrum of a signal record is shown in Figure 5. At this point, the signal is now represented by a Fourier Series expansion and has the form

$$e(t) = \sum_{m=-n}^n C_n e^{j(\phi_n)} e^{jn\omega_0 t}$$

where  $C_n$  is the amplitude of a vector rotating at a frequency  $n\omega_0$  with a phase angle  $\phi(n)$ . The power spectrum is a plot of  $C^2(n\omega_0)$  vs  $n\omega_0$ . The value  $n\omega_0$  is the frequency of the sinusoid. The phase spectrum is a plot of the phase  $\phi(n\omega_0)$  of the signal vector with respect to the reference vector vs frequency. Since these spectra constitute only a set of discrete values, they are line spectra and frequencies between the lines have no meaning. The spectra of Figures 4 and 5 are shown as continuous spectra which they are not and are shown this way only for presentation purposes. Even though the spectra shown are line spectra, for frequencies below the Nyquist point, they constitute an exact representation of the input digital signal with the exception of grain noise at high spatial frequencies which is folded over to the signal part of the spectrum by the sampling process. However, this is minimized by the spatial filtering process in the transform phase of the optical correlator.

After the phase spectrum is obtained for an individual record, the phase spectrum is corrected for the system frequency dispersion which is, by design, a quadratic function of frequency. The phase spectrum of Figure 5, after the quadratic phase correction, now looks as that shown in Figure 6. The transform of this phase spectrum and the amplitude spectrum represents a digitally compressed signal record as shown in Figure 7. Before the phase spectrum can be rolled back to the reference plane, the range to the reference plane must be estimated and this is done by synthesizing the new signal from the new

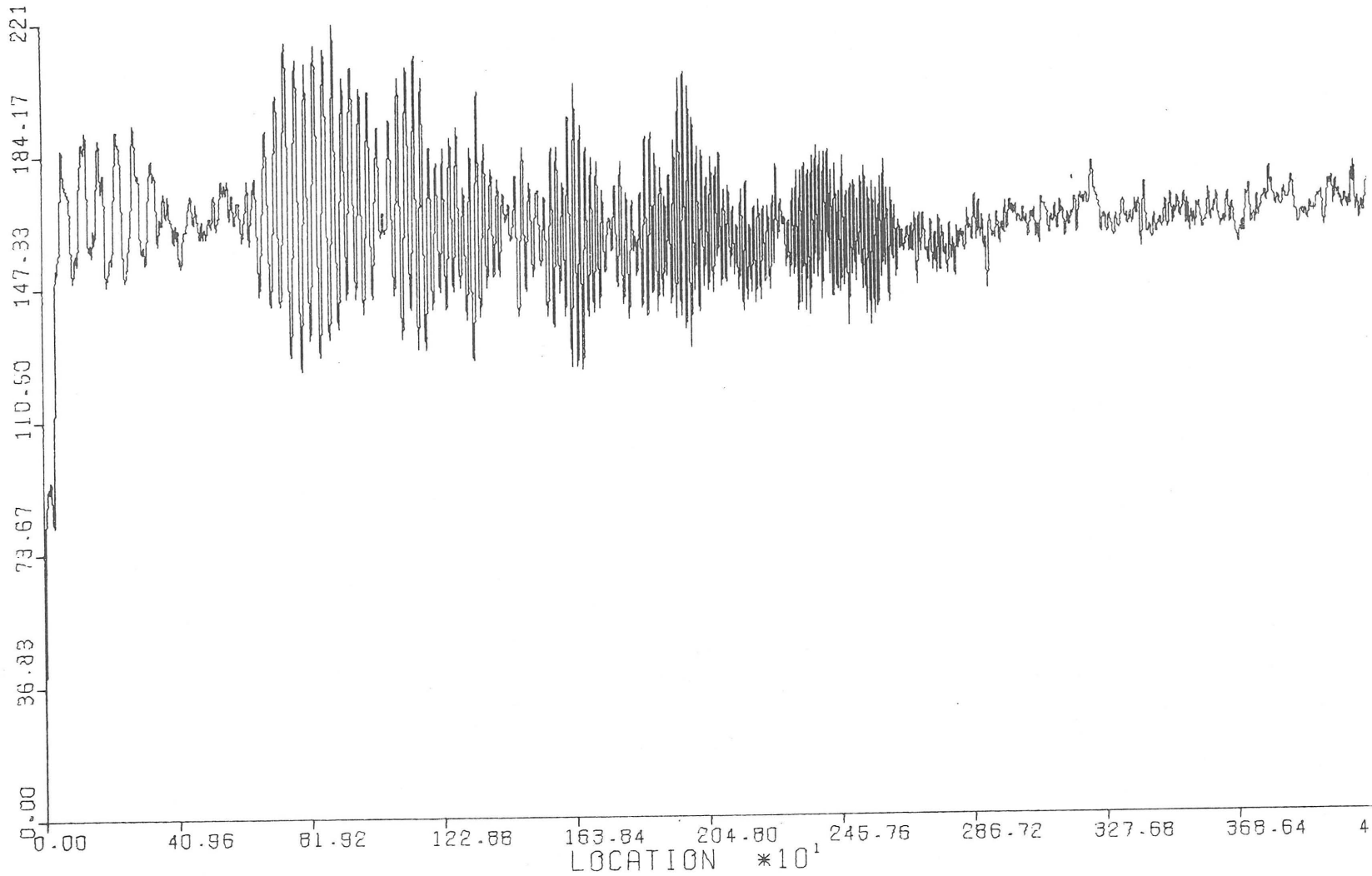


Figure 3. Microdensitometer Trace of a Doppler Filtered Linear Signal Record



13

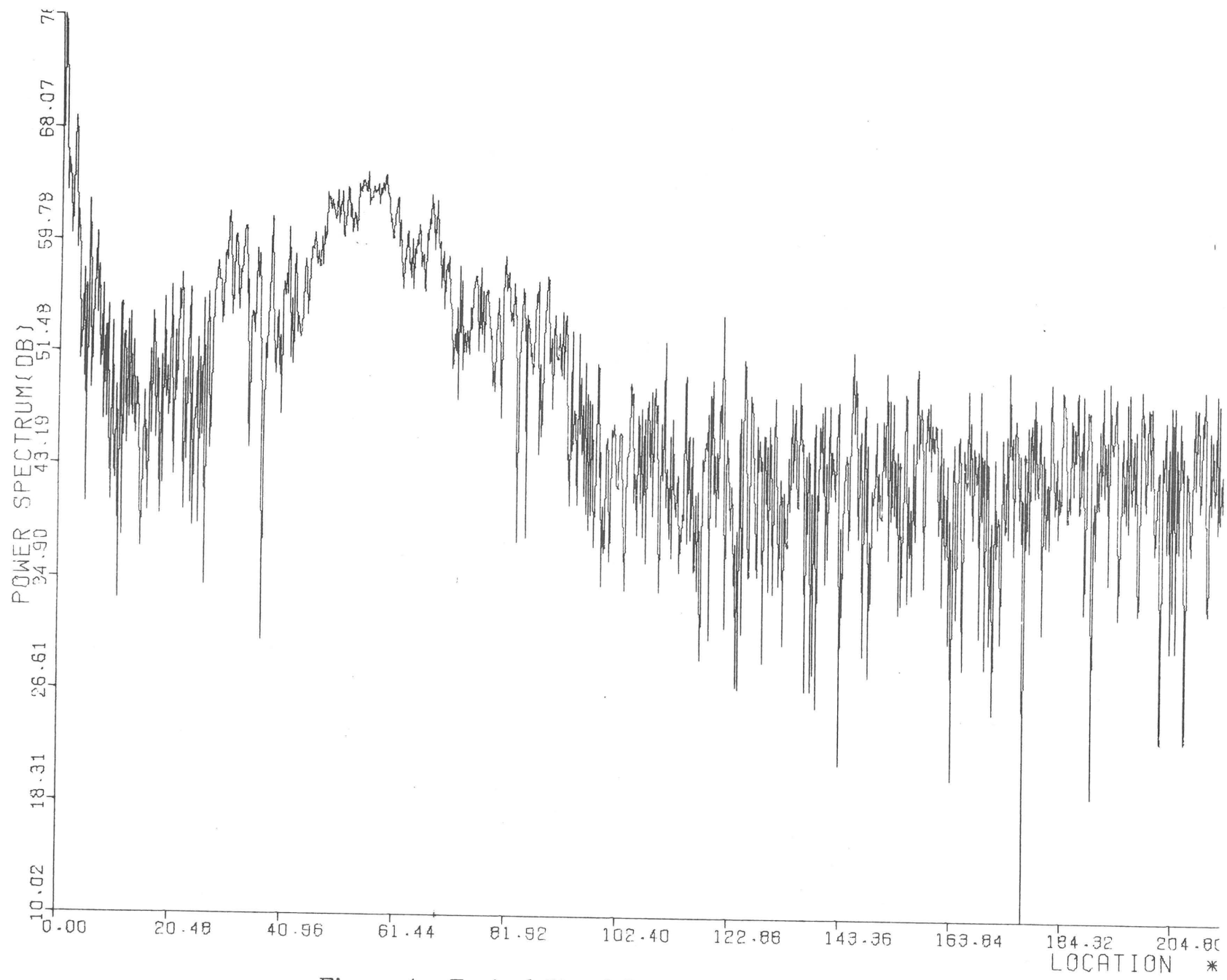


Figure 4. Typical Signal Record Power Spectrum

609-51

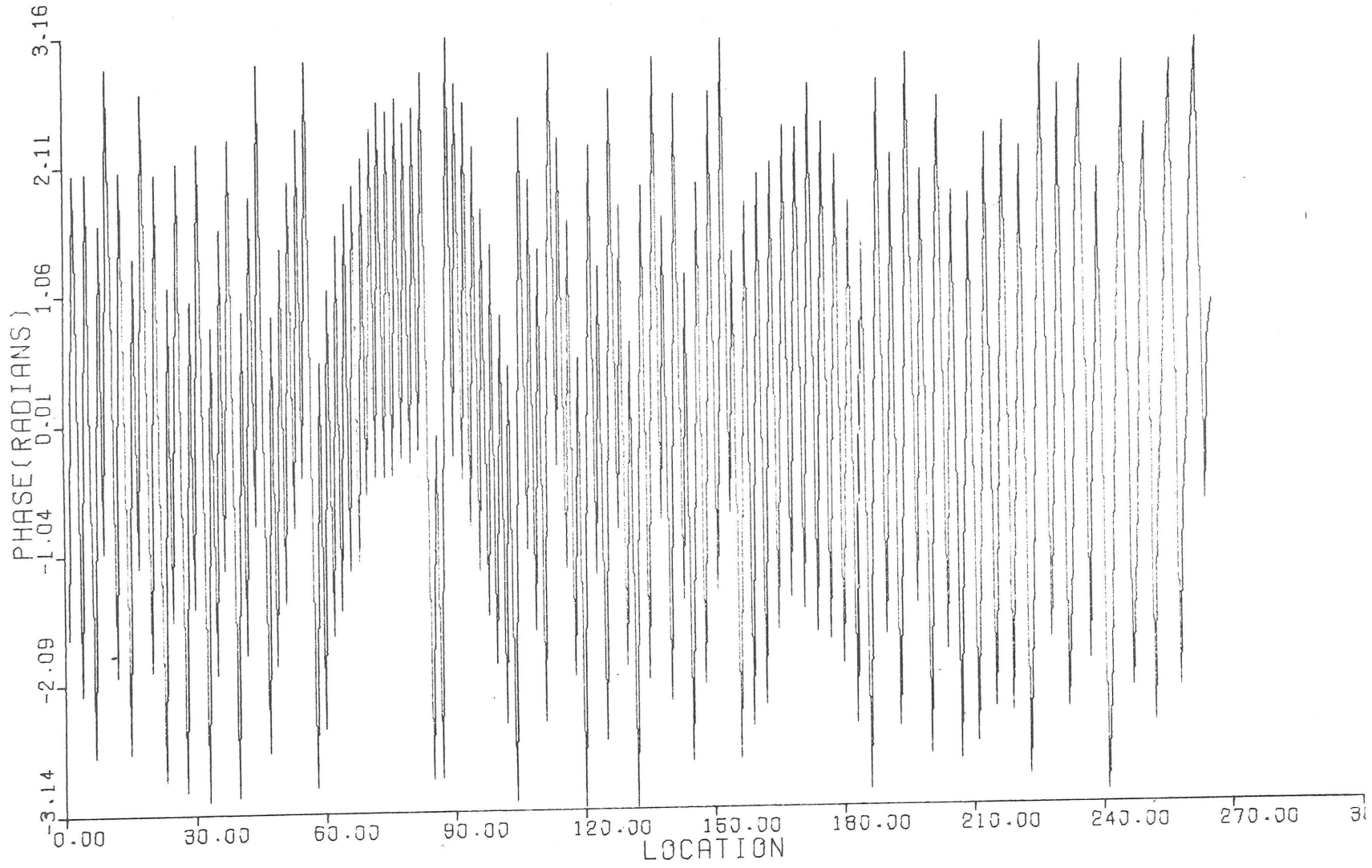


Figure 5. Typical Signal Record Phase Spectrum

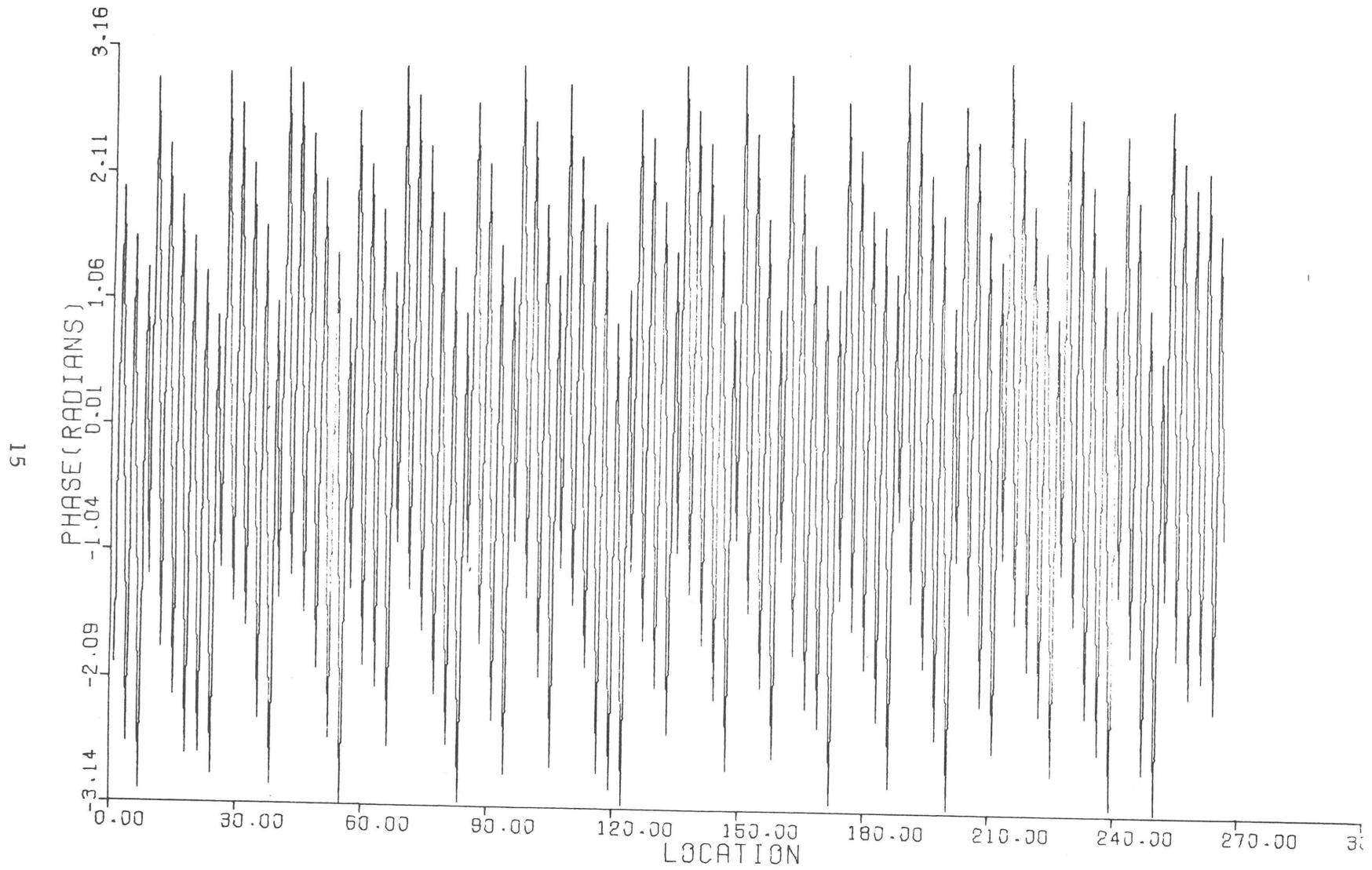


Figure 6. Typical Signal Record Phase Spectrum after Quadratic Phase Correction

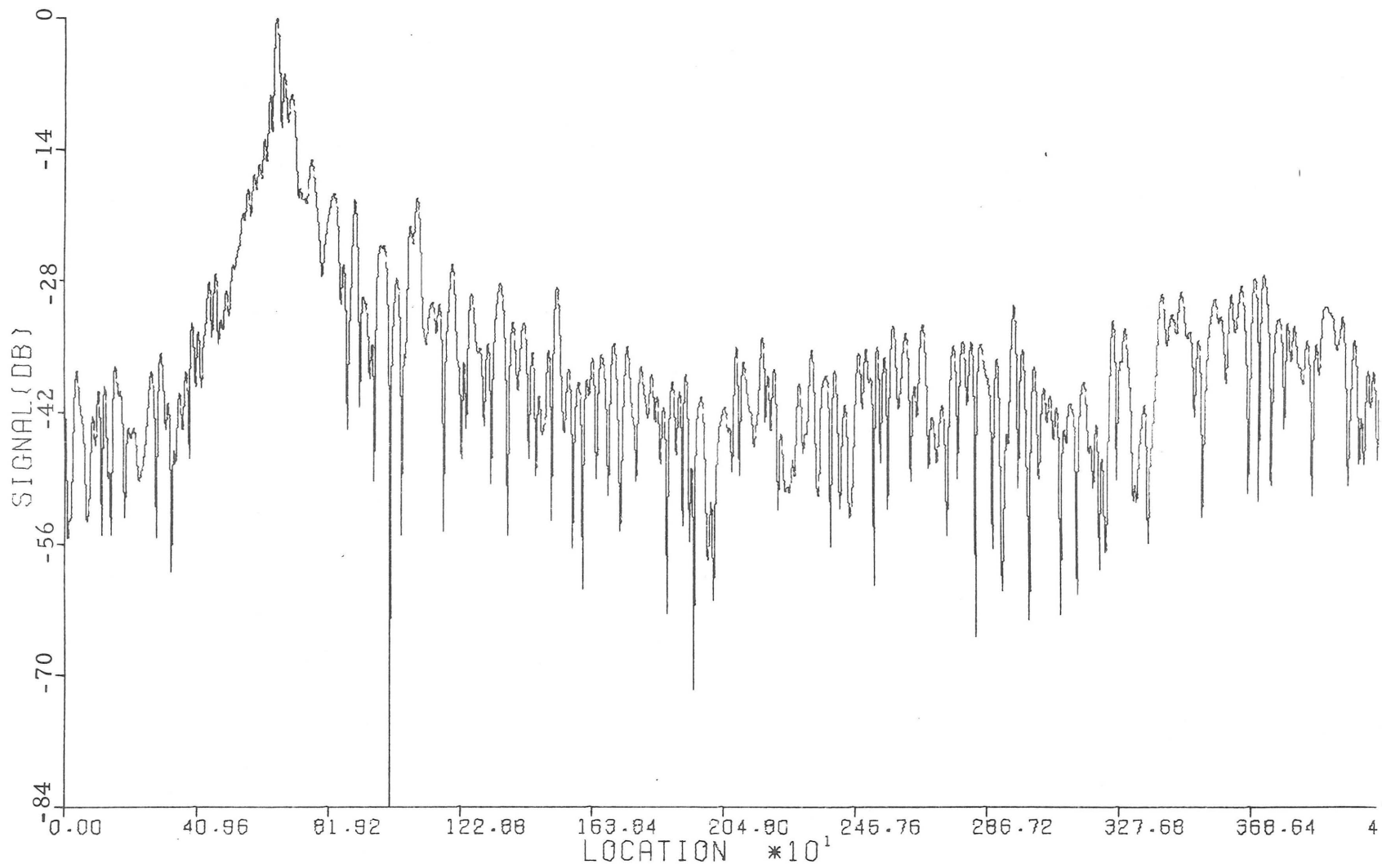


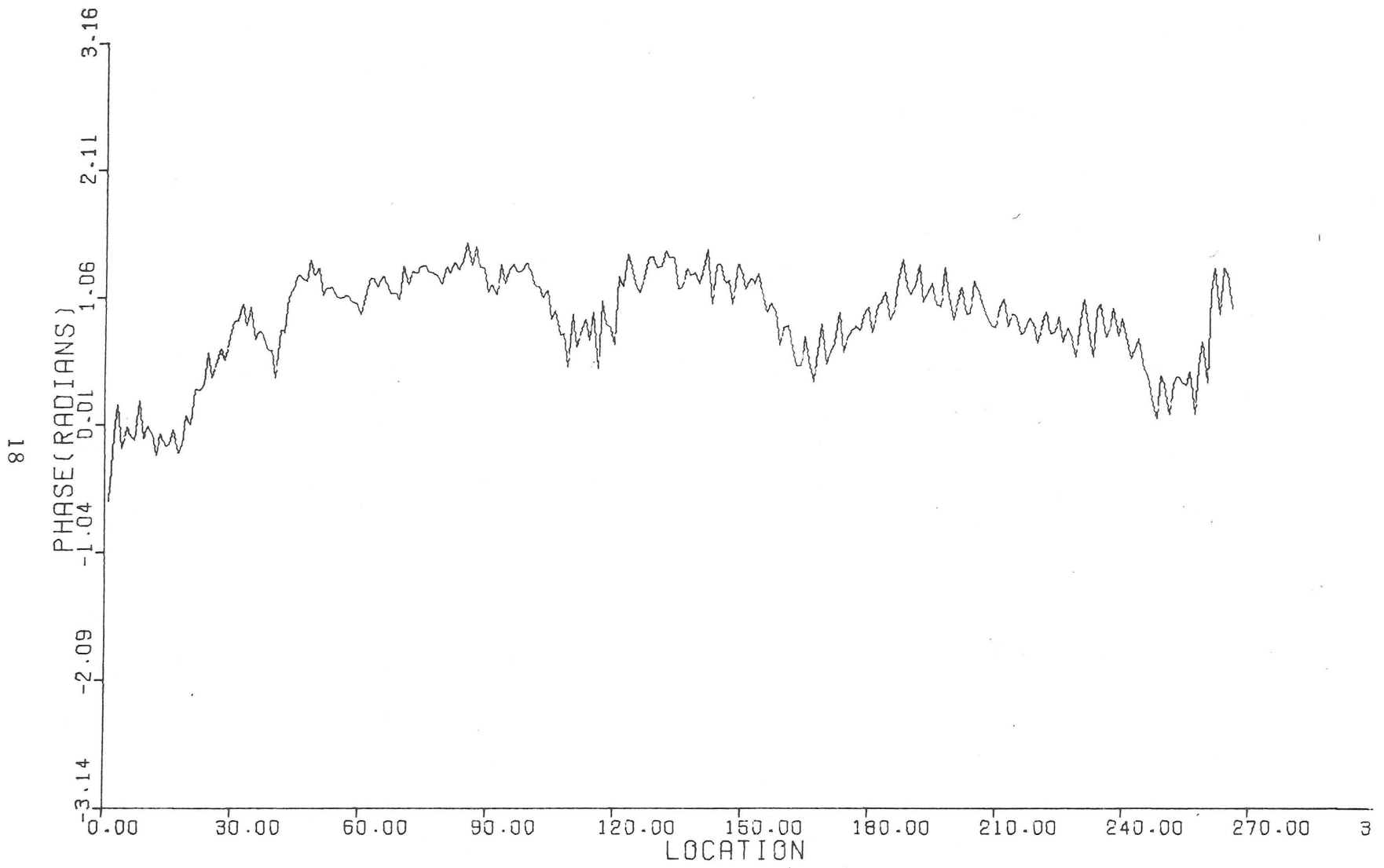
Figure 7. Typical Signal Record after Pulse Compression

Fourier Series expansion and locating its peak. When the peak has been located, each sinusoid of the frequency series expansion is advanced in phase an amount corresponding to this shift in temporal location. The result is a phase spectrum as shown in Figure 8. The amplitude spectrum is, of course, unchanged as the operations that we are performing are purely those corresponding to shifts in location. At this point, a rotation in the reference plane is made to center the spectrum about the zero phase line and a final shift in location of reference plane is made by filtering the phase spectrum to a least squares error fit to a first degree polynomial, and taking the difference between the phase line spectrum and the fitted line. In effect, we have precisely located the center of the reflection point with respect to the initial digitized point on the film. The accuracy which we have been able to accomplish this on lunar data for HF1 is 0.7 microns, which corresponds to 3 degrees of the center frequency. This corrected spectrum now looks like that shown in Figure 9.

This procedure is repeated for a number of signal records. Some records will contain either too much noise, too much clutter (multiple returns) or too much higher order harmonics. Records whose referenced phase spectra meet the selected criteria are then preserved for stacking. After stacking a number of these spectra, the resultant spectrum begins to integrate in towards the system phase error since noise and clutter do not have frequency and time invariant phase spectra. The result then is as shown in Figure 10. The weighted transform of this phase spectrum is then the time invariant system sidelobe function and is as shown in Figure 11.

#### 4.0 CONCLUSIONS

A section of ALSE signal film was digitized and analyzed in order to investigate the feasibility of this technique. The section digitized was the 40 seconds of HF1 data following the start of FT01. The digitizer characteristics were set at a 10 micron spacing in range, and an aperture of 20 by 320 microns in range and azimuth, respectively. The resultant processing parameters are tabulated in Figure 12. After digitization, each record was run through the previously mentioned program to obtain the Fourier transforms of the individual records as well as the "stacked" amplitude and phase spectra. The resulting stacked phase spectrum is shown in Figure 10 and the stacked amplitude spectrum in Figure 13. Since the amplitude spectrum thus obtained



609-51

Figure 8. Typical Phase Spectrum after Quadratic Phase Correction and Initial Phase Rollback

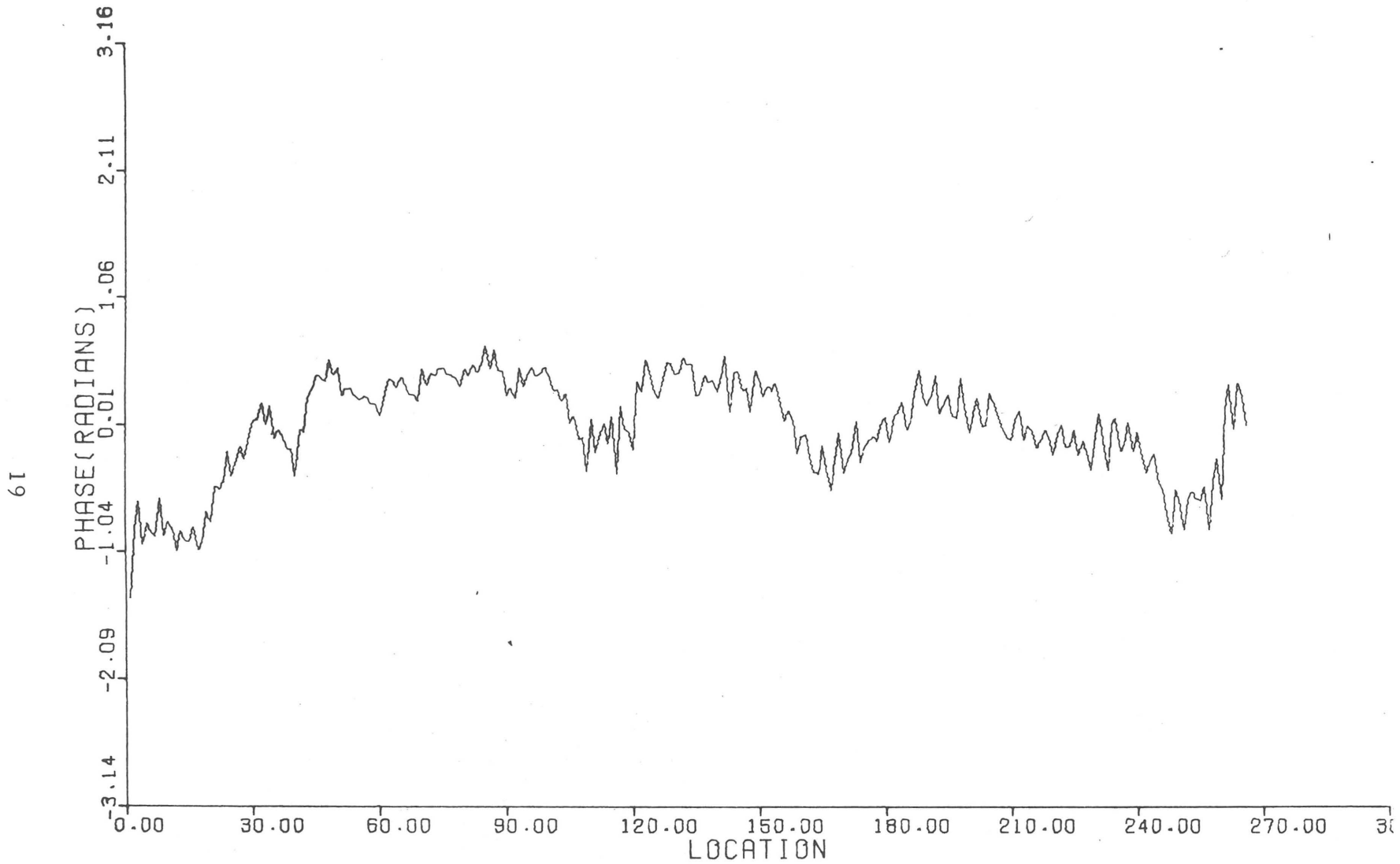
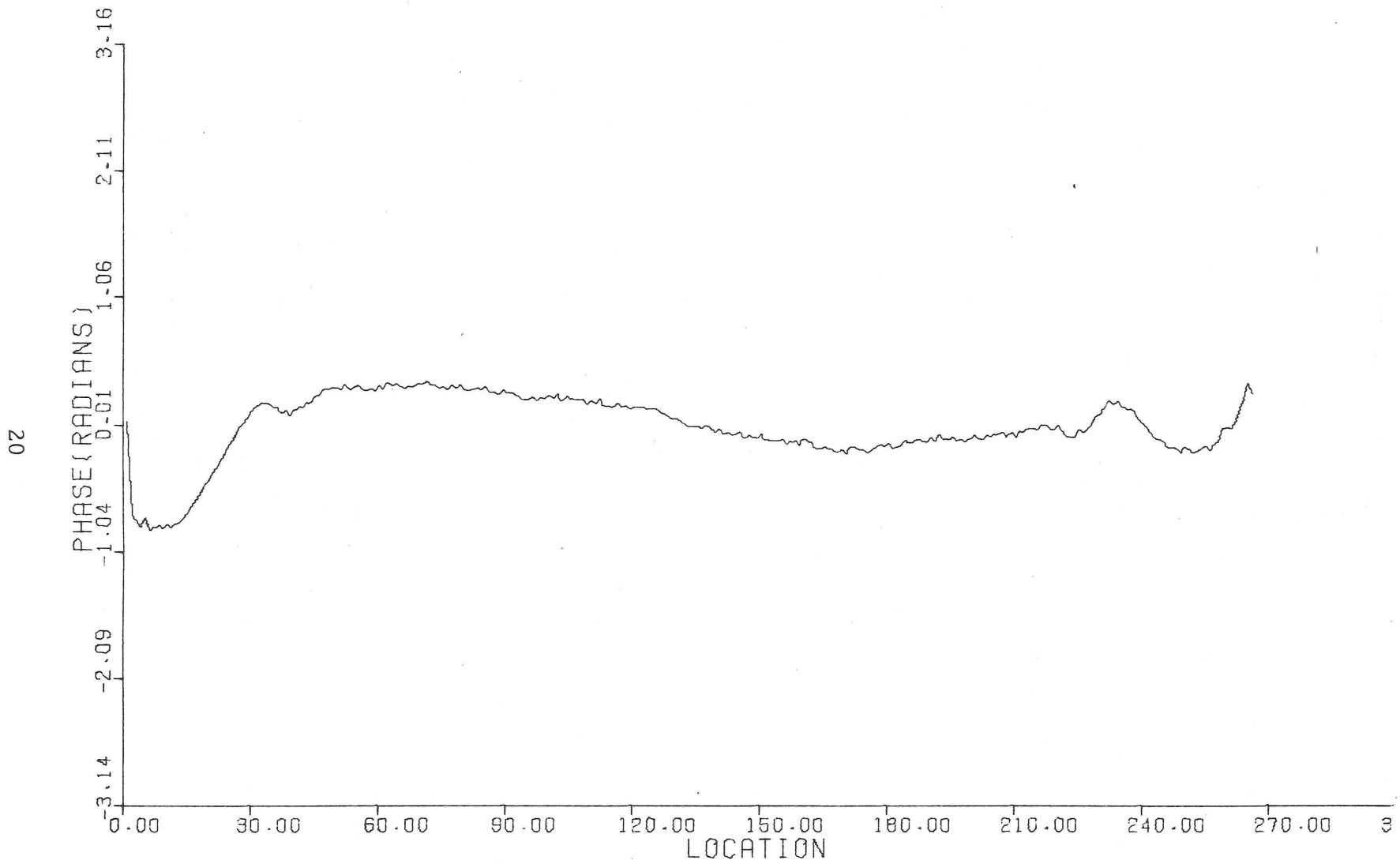


Figure 9. Typical Phase Spectrum after Quadratic Phase Correction and Rotation.  
This Spectrum is Ready for the Stacking Operation.



609-51

Figure 10. System Phase Error Function



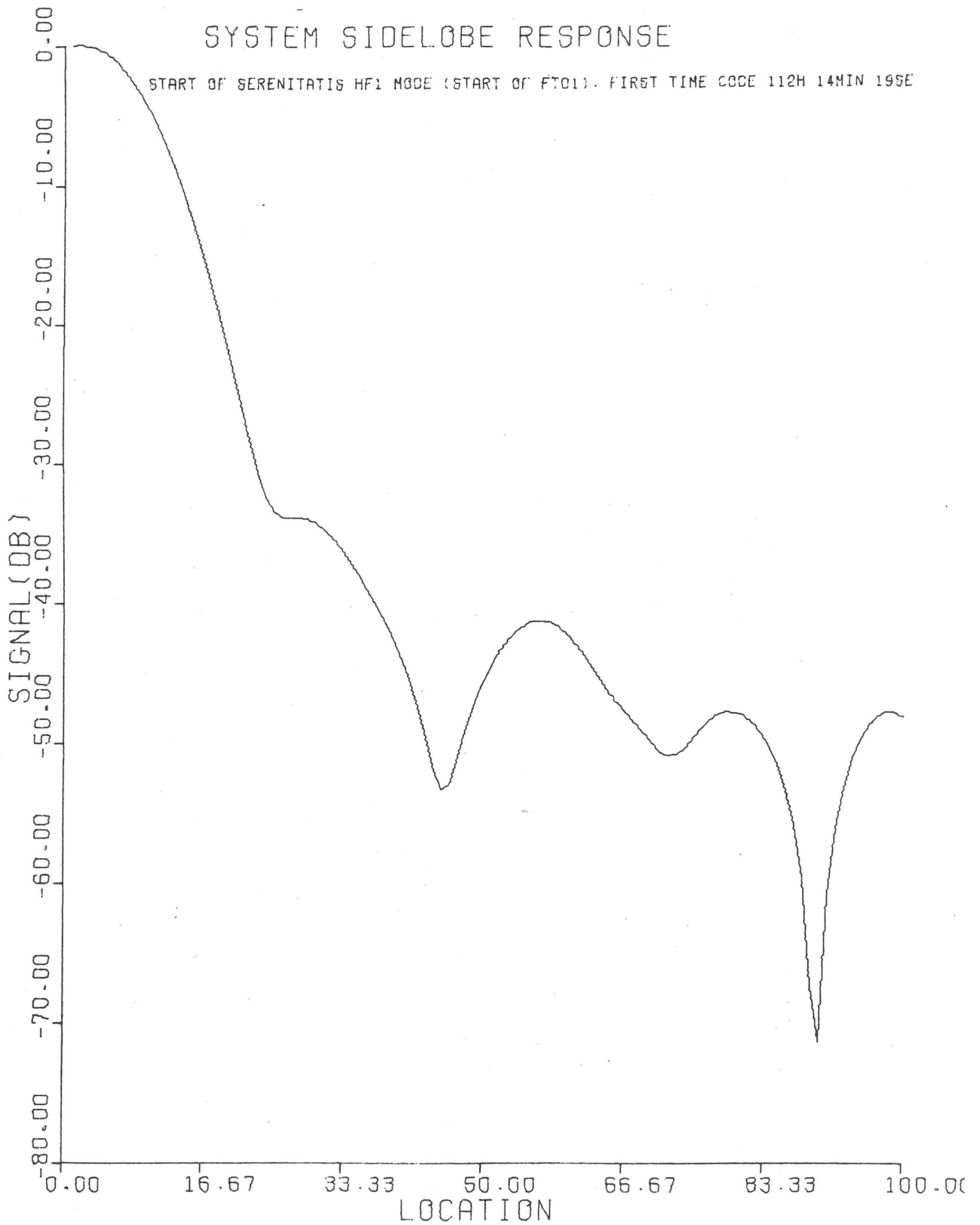


Figure 11. System Sidelobe Response with  $\text{Sinc}^2$  Weighting

## RADAR DATA PARAMETERS

## HF1 SYSTEM

## DIGITIZER CHARACTERISTICS

SAMPLE SPACING	=	10.00 MICRONS
X APERTURE	=	20.00 MICRONS
Y APERTURE	=	320.00 MICRONS

## EQUIVALENT PROCESSING PARAMETERS

SAMPLE TIME INCREMENT	=	.2427-06 SECONDS
SWEEP VELOCITY	=	41.20 METERS/SEC
FREQUENCY INCREMENT	=	2011.9 CPS
LOWER LIMIT	=	231
UPPER LIMIT	=	761
NUMBER OF FREQUENCIES	=	266
DISPERSION CONSTANT	=	.4112+07
FILM WIDTH	=	.025 METERS
SWEEP DURATION	=	606.734 MICROSECONDS
BANDWIDTH	=	.533 MHZ
LOW FREQUENCY	=	.231 MHZ
HIGH FREQUENCY	=	.765 MHZ
WIDTH DIGITIZED	=	20.480 MM.
RADAR SPACE COVERED	=	74.555 KILOMETERS
SAMPLE POINTS	=	2048
LOW SPATIAL FREQUENCY	=	5.62 CYCLES/MM
HI SPATIAL FREQUENCY	=	18.55 CYCLES/MM
X APERTURE CUTOFF	=	50.00 CYCLES/MM
Y APERTURE CUTOFF	=	3.13 CYCLES/MM
RANGE NYQUIST FREQ	=	50.00 CYCLES/MM
3 DB HALF BEAMWIDTH	=	7.95 DEGREES

Figure 12. Radar Data Parameter Tabulation

consists of the overall system amplitude spectrum convolved with the digitizer window characteristics, the system amplitude spectrum may be obtained by deconvolving these functions. The resultant system amplitude spectrum is shown in Figure 14. The effects of the Fresnel ripples may be seen as well as the distinct fall off due to probably the recorder MTF. From this amplitude and phase spectra, the system sidelobe response may be calculated and a printer plot of this response is shown in Figure 15. After performing a sinc squared weighting operation, the sidelobe response is shown in Figure 16. This may be compared with the "perfect" system response shown in Figure 17 after the same sinc squared weighting.

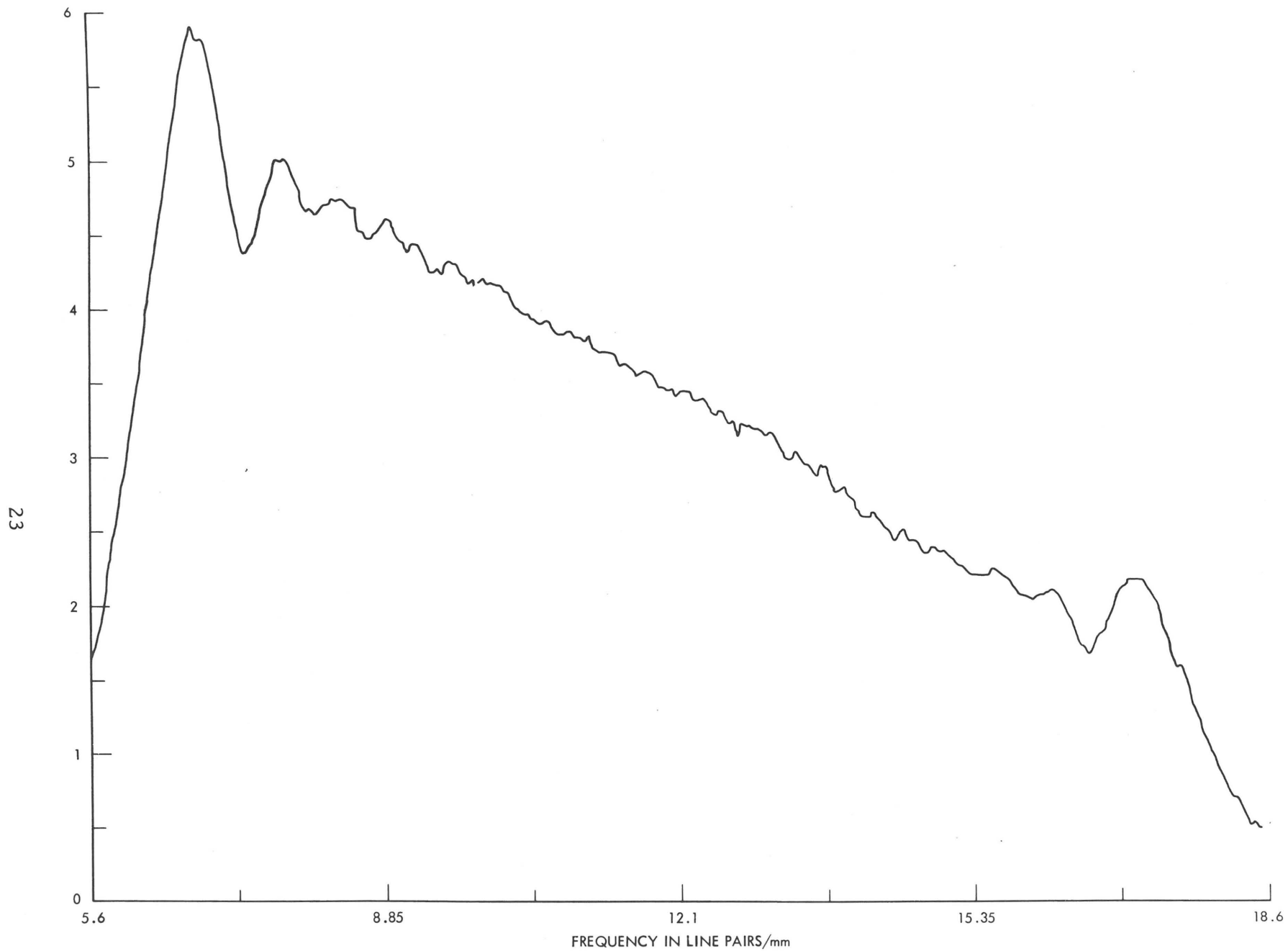


Figure 13. Relative Amplitude Spectrum of HF1 ALSE Data (Start of FT01)

609-51

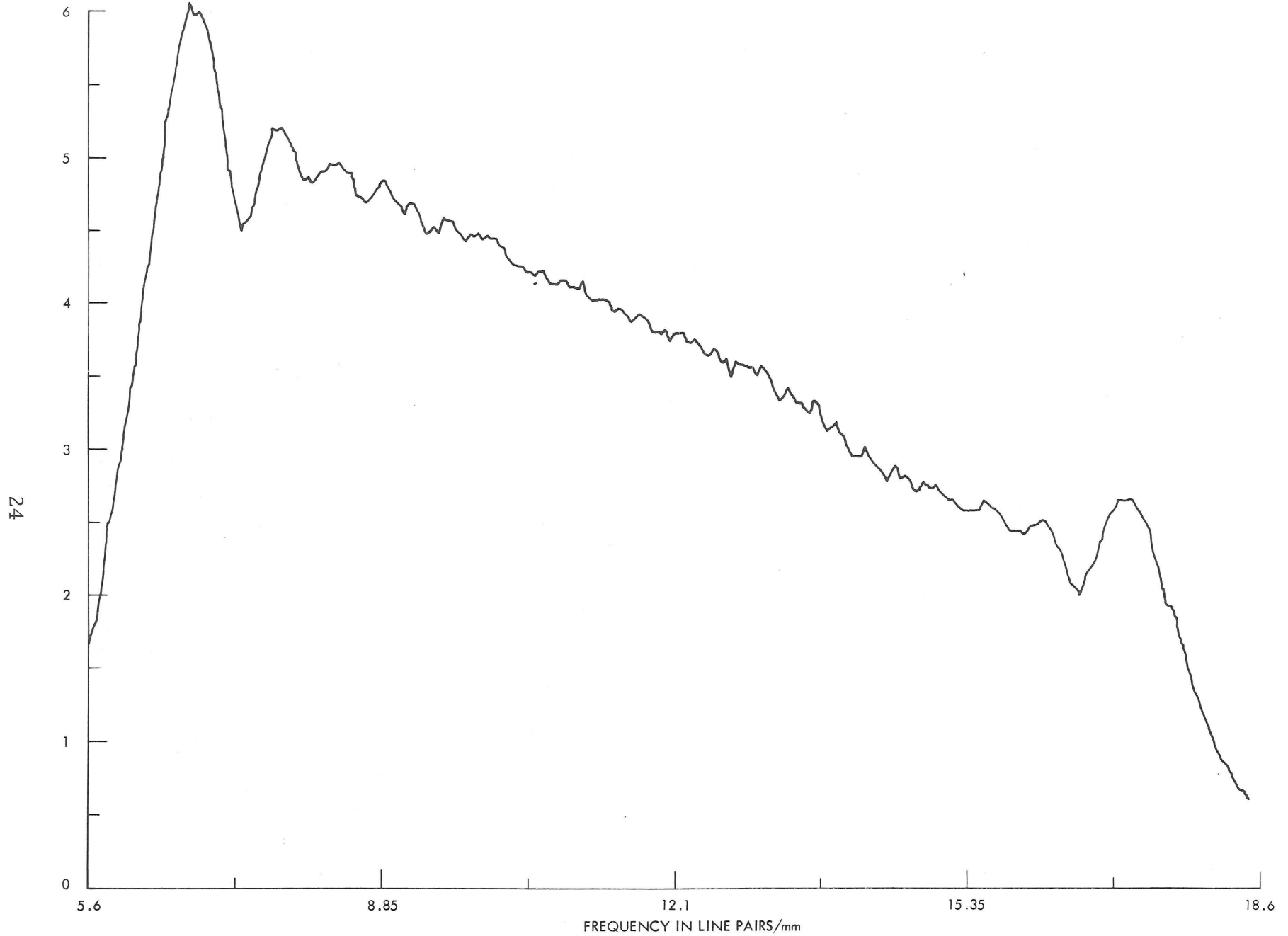


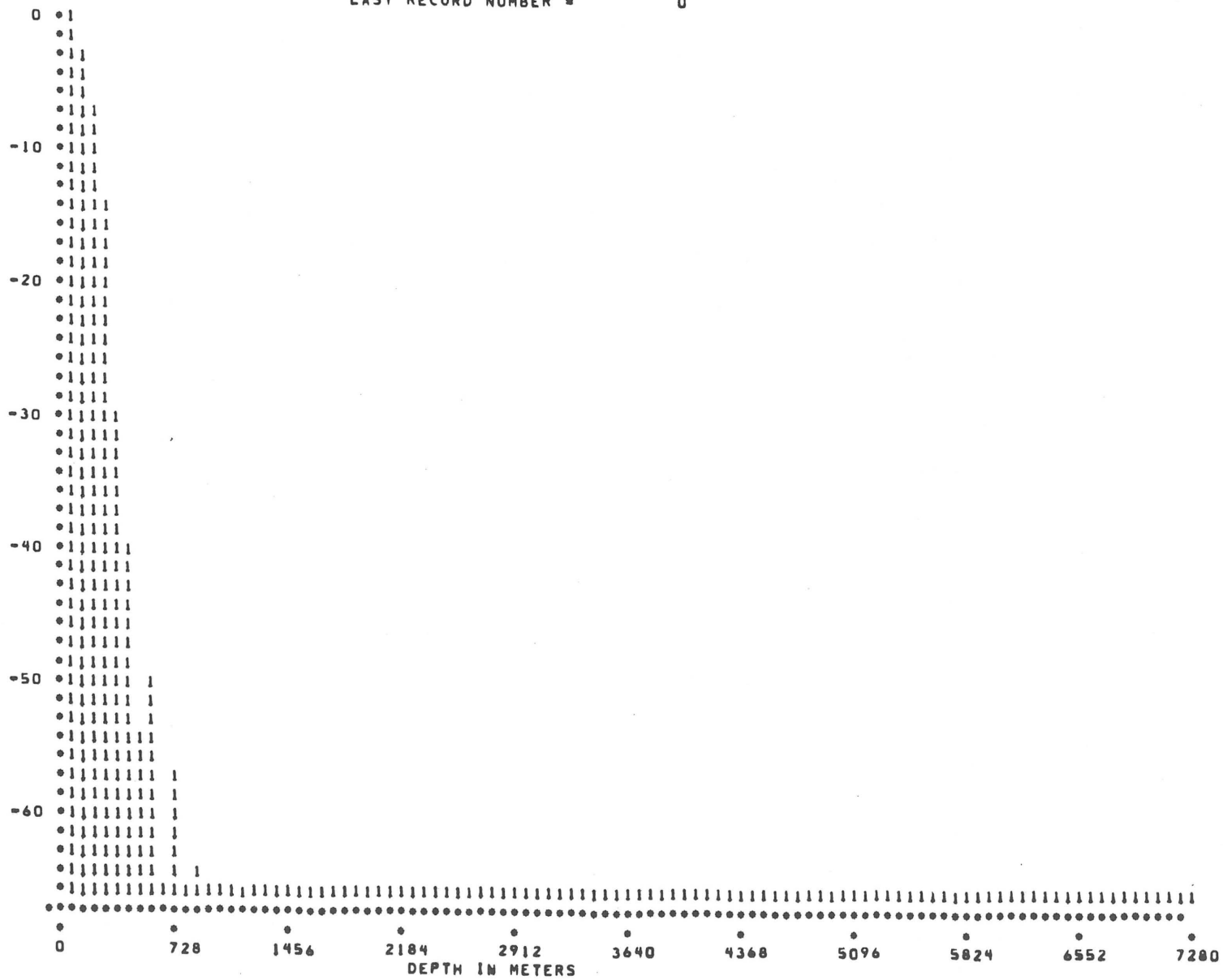
Figure 14. ALSE HF1 System Relative Amplitude Spectrum

609-51





WEIGHTED SIDELobe RESPONSE  
LAST RECORD NUMBER = 0



27

609-51

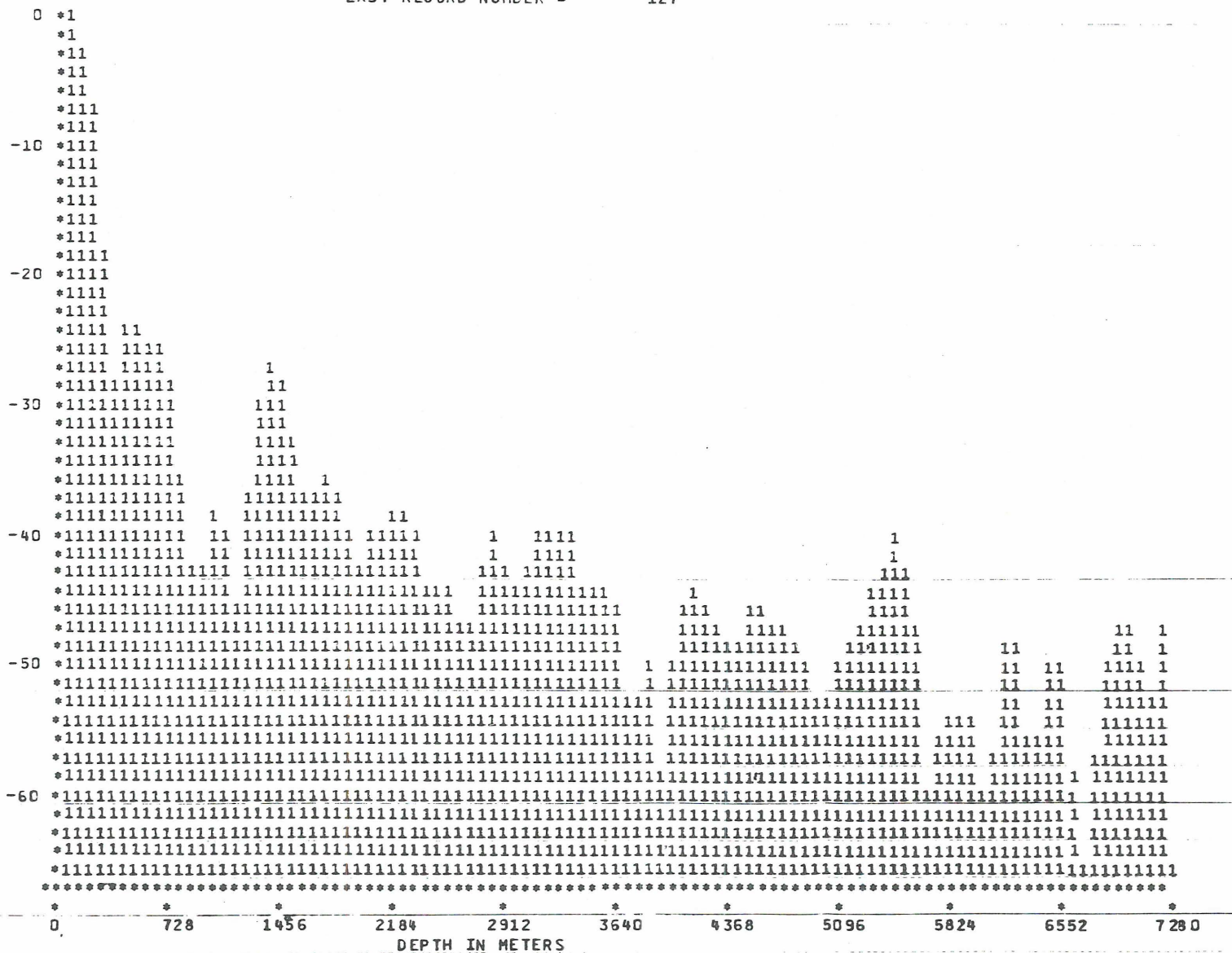
Figure 17. Ideal System Sidelobe Response

If a single record is deconvolved with the system response function and the compressed, weighted time response examined, the resultant positive time plot is as shown in Figure 18. As can be seen, the response at times corresponding to depths greater than the system resolution is significantly greater than the system sidelobe response due to excess positive time returns (clutter or subsurface features). Thus, for a coarse analysis without coherent azimuth stacking, it is not necessary to perform a digital correction to the system response. However, as the number of echoes stacked increases, this clutter or noise comes down, depending on the number of stacked pulses. The stacked returns after 64 stacks is shown in Figure 19 and, after 512 stacks, in Figure 20. It can be seen that the system dynamic range greatly increases (as would be expected) after coherently stacking these returns and that this technique becomes necessary if the returns to be examined are greater than 45 to 50 db below the surface return. The process used after obtaining the system amplitude and phase spectra may have to be further refined to optimally process for different geologic models. However, for processing for parallel layers to the surface, this technique is necessary to look for very weak returns.





WEIGHTED SIDELobe RESPONSE  
 LAST RECORD NUMBER = 127

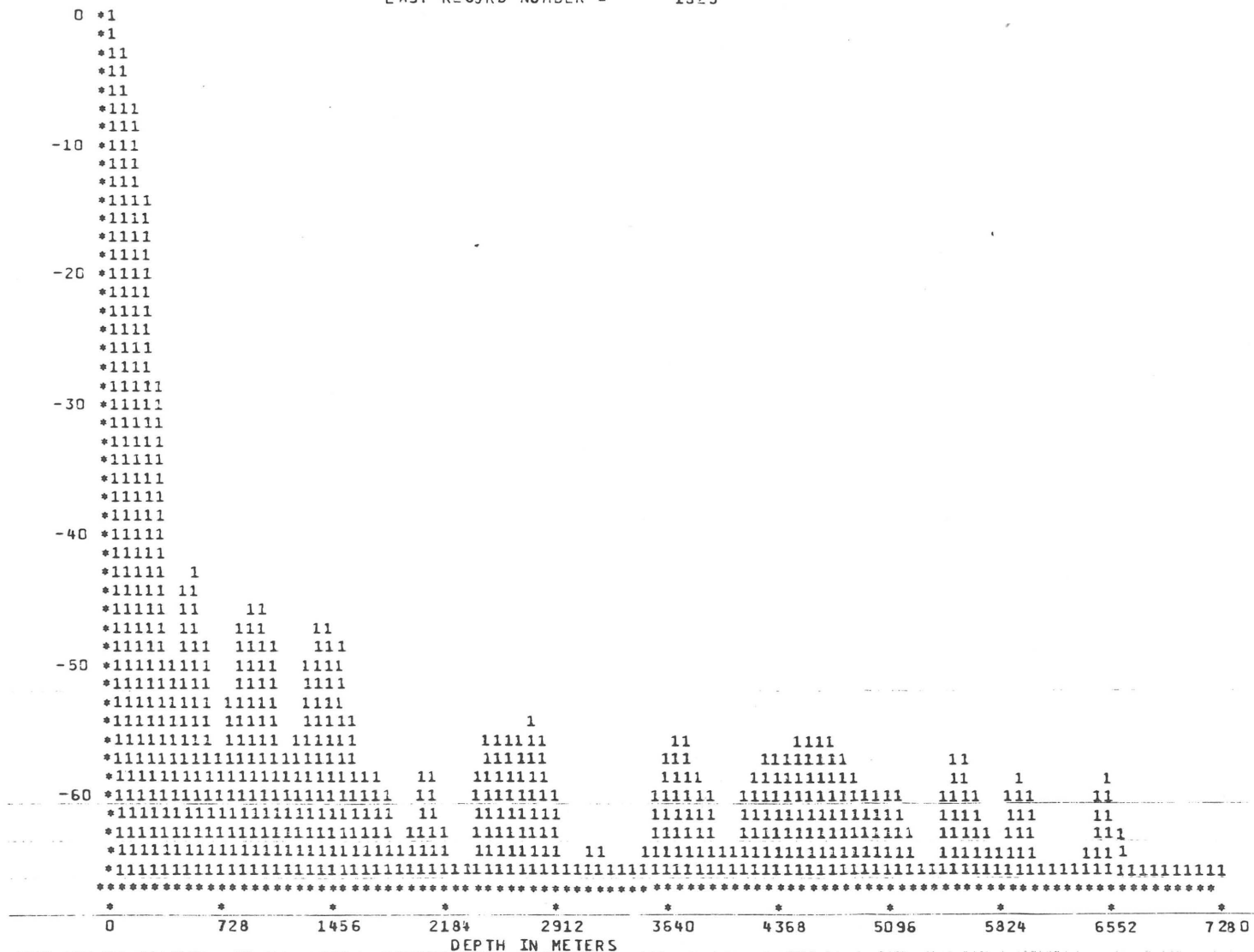


30

609-51

Figure 19. Pulses Stacked = 64

WEIGHTED SIDELobe RESPONSE  
 LAST RECORD NUMBER = 1023



WEIGHTED SIDELobe RESPONSE

Figure 20. Pulses Stacked = 512